Orientational relaxation of liquid water molecules as an activated process

Han-Kwang Nienhuys[a)]
FOM Institute for Atomic and Molecular Physics, Kruislaan 407, 1098 SJ Amsterdam, The Netherlands and Schuit Catalysis Institute, Eindhoven University of Technology, P.O. Box 513, 5600 MB Eindhoven, The Netherlands

Rutger A. van Santen
Schuit Catalysis Institute, Eindhoven University of Technology, P.O. Box 513, 5600 MB Eindhoven, The Netherlands

Huib J. Bakker
FOM Institute for Atomic and Molecular Physics, Kruislaan 407, 1098 SJ Amsterdam, The Netherlands

(Received 8 July 1999; accepted 25 February 2000)

Femtosecond mid-infrared pump–probe spectroscopy is used to study the orientational relaxation of HDO molecules dissolved in liquid D_2O. In this technique, the excitation of the O–H stretch vibration is used as a label in order to follow the orientational motion of the HDO molecules. The decay of the anisotropy is nonexponential with a typical time scale of 1 ps and can be described with a model in which the reorientation time depends on frequency and in which the previously observed spectral diffusion is incorporated. From the frequency and temperature dependence of the anisotropy decay, the activation energy for reorientation can be derived. This activation energy is found to increase with increasing hydrogen bond strength. © *2000 American Institute of Physics.* [S0021-9606(00)52019-4]

I. INTRODUCTION

Water is undoubtedly a liquid that is very important to (bio)chemistry. It exhibits remarkable properties due to the high density of hydrogen bonds. Although water has been studied in great detail since a long time, the microscopic dynamics, such as vibrational relaxation and the thermal motion of the molecules, could not be investigated experimentally due to the strong inhomogeneity of water and the ultrafast time scale on which these processes take place. Fortunately, it has recently become possible to study these processes in detail thanks to the development of lasers that deliver intense femtosecond mid-infrared pulses.

Recently, in a study where 250 fs mid-infrared pulses were used, it was found that the orientational motion of HDO molecules in D_2O at room temperature could be described with two distinct time constants of 700 fs and 13 ps.[1] It was found that the component with a time constant of 700 fs predominantly absorbs at the high-frequency side ($3500\,cm^{-1}$) of the O–H stretch absorption band, and that this component is completely absent at the low-frequency side of the absorption band. In another recent study, it was found that the reorientational time constant varied from 3 ± 1.5 ps at $3500\,cm^{-1}$ to 13 ± 5 ps at $3330\,cm^{-1}$.[2] In this study, however, 2 ps pulses were employed, which renders the determination of short time constants more difficult.

The frequency of the O–H stretch vibration is strongly determined by the length of the O–H···O hydrogen bond between the hydrogen atom of the O–H group and the oxygen atom of a neighboring water molecule; the shorter the distance, the lower the frequency.[3] Hence, the observation of a slow reorientational component at the red side and a fast component at the blue side shows that the orientational motion is strongly influenced by the hydrogen bond strength.

In this paper, we present a detailed study on the orientational motion of HDO molecules in liquid D_2O. We describe the experimental results with a model that includes the effects of spectral relaxation. By varying the temperature, we obtain information on the activation energy that limits the rate of reorientation.

II. EXPERIMENT

A. Infrared generation

Figure 1 shows the pulse-generation setup. The infrared laser pulses used in our experiments were generated by a Ti:sapphire regenerative amplifier (RGA) system at 800 nm, followed by two optical parametric generation and amplification stages (OPG/OPA). We used a commercial RGA that generates 800 nm, 150 fs, 1 mJ pulses at a 1 kHz repetition frequency. In the first OPG/OPA stage, based on a β-barium borate (BBO) crystal, the 800 nm pulses are partially converted to infrared pulses with typical central wavelengths of 1140 nm (signal) and 2650 nm (idler). Due to absorption in BBO, no larger idler wavelengths can be generated. However, the 1090 nm wavelength, that is complementary to 3000 nm in the idler, is present within the bandwidth of the signal pulse. In the second stage, this broadband signal is used as seed in an OPA process in a potassium titanyl phosphate (KTP) crystal that is pumped by the remaining 800 nm light. This yields an idler at 3000 nm. The idler wavelength can be continuously tuned up to 3300 nm and typically has an energy of 20 μJ, a bandwidth of 80 nm and a full width at half maximum duration of 250 fs. This maximum wavelength corresponds to a minimum frequency of $3000\,cm^{-1}$, which is suitable for exciting and probing the O–H stretch

a)Electronic mail: h.nienhuys@amolf.nl

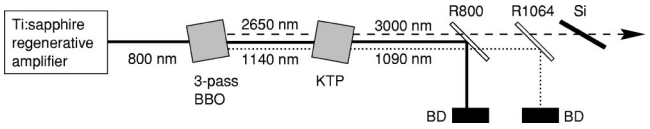

FIG. 1. Generation of 3 μm pulses. Abbreviations: BBO: BBO crystal; KTP: KTP crystal; R800: dielectric 800 nm mirror; R1064: dielectric 1064 nm mirror; Si: silicon Brewster window; BD: beam dump.

vibration in water (see Fig. 2). The remaining pump and signal wavelength components are removed by means of dielectric 800 and 1064 nm mirrors. Any remaining short wavelength components are filtered out by a silicon plate positioned at the Brewster angle. The infrared pulse generation is described in more detail elsewhere.[4]

B. Pump–probe setup

Figure 3 shows a schematic outline of the pump–probe setup. Part of the pulse energy is split off by an uncoated and wedged CaF_2 window, which yields a pump, a probe and a reference beam. The probe and pump pulses are focused to a 200 μm wide spot in the sample. Using PbSe photoconductive cells, we measure the energy of the light pulses transmitted through the sample, and the energy of the pulses in the reference beam, in order to compensate for pulse-to-pulse energy fluctuations. By using a chopper to block every other pump pulse, we obtain both the transmission T in the presence of a pump pulse, and the reference transmission T^0. Thus we can calculate the absorption change $\Delta\alpha = -\ln(T/T^0)$ as a function of the delay between the pump and probe pulses.

The pulse frequency is tuned within the absorption band of the O–H stretch vibration (see Fig. 2). The pump pulse excites part of the population of molecules to the excited $v=1$ vibrational state. Since this excitation is a dipole transition, the excitation preferentially takes place for molecules that have their O–H bond parallel to the pump light polarization. Directly after excitation, the population of excited molecules per unit of solid angle will be proportional to $\cos^2\theta$, where θ is the angle between the O–H bond and the pump polarization. Due to this anisotropic population of excited molecules, the absorption change $\Delta\alpha_\parallel$ for the case where the probe polarization is parallel to the pump polarization will be larger than the absorption change $\Delta\alpha_\perp$ for the case where the probe polarization is perpendicular to the pump polarization. From $\Delta\alpha_\parallel$ and $\Delta\alpha_\perp$, we can calculate the rotational anisotropy[5]

$$R=\frac{\Delta\alpha_\parallel-\Delta\alpha_\perp}{\Delta\alpha_\parallel+2\Delta\alpha_\perp}. \tag{1}$$

The denominator here corresponds to the isotropic absorption change, that is not affected by reorientation. For the initial $\cos^2\theta$ distribution, it can be shown that $R=2/5$. As this highly anisotropic distribution becomes more and more isotropic as a result of reorientation of the individual HDO molecules, the value of R decays to zero. By measuring R as a function of the delay between pump and probe pulses, we obtain information on the orientational motion of the HDO molecules. It should be noted that R is not affected by the relaxation of excited molecules to the ground state, since this affects the numerator and the denominator in Eq. (1) in the same way.

In order to measure $\Delta\alpha_\parallel$ and $\Delta\alpha_\perp$, the polarization of the probe is rotated over 45° with respect to the pump polarization by using a $\lambda/2$ plate. The polarization components of the probe light that are parallel and perpendicular to the pump light are detected independently by means of a beamsplitter and two polarizers behind the sample.

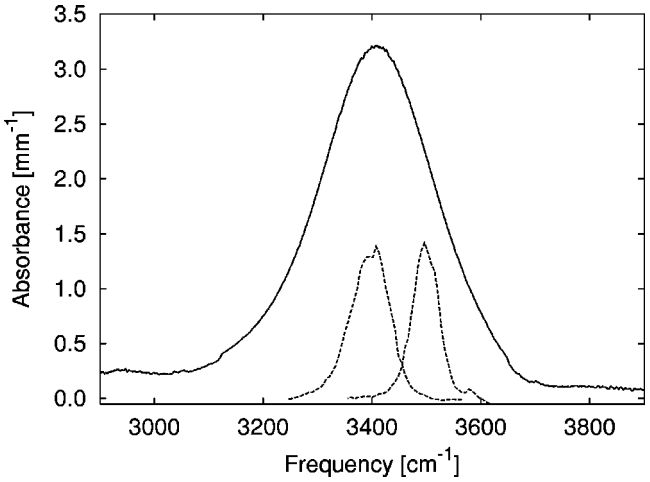

FIG. 2. Absorption spectrum of a 0.4% HDO in D_2O solution (solid line), with the pulse spectra (dashed lines).

C. Data acquisition

The parametric generation and amplification process that we use to obtain infrared pulses, is inherently a source of noise in the signals being measured. Since the conversion process depends highly nonlinear on the energy of the pump pulses, any fluctuations in the 800 nm pump energy show up as large variations in the energy of the infrared pulses at 3 μm. It is not uncommon to observe an individual pulse energy that differs by 30% from the average pulse energy. In addition, the power spectrum and the beam profile can vary slightly from pulse to pulse. Therefore, it is important to design the experiment such that an optimal signal to noise ratio is achieved.

In order to correct for energy fluctuations, we use one detector to measure the energies of the pulses in the reference beam. In the case of the laser shots where a pump pulse is present, this yields reference energies r_i, where the subscript $i=1,\ldots,N$ indicates the individual pulses. Two other detectors acquire the energies $p_{\parallel,i}$ for the parallel and $p_{\perp,i}$ for the perpendicular components of the probe pulses after the sample. For the laser shots without a pump pulse, the energies are r_i^0, $p_{\parallel,i}^0$, and $p_{\perp,i}^0$, as indicated by the zero superscript. Then, the transmissions are $T_{\varepsilon,i}=p_{\varepsilon,i}/r_i$ and $T_{\varepsilon,i}^0=p_{\varepsilon,i}^0/r_i^0$, where ε indicates the polarization. (Formally, this is not correct if the detectors have different efficiencies. However, this does not affect the ratio $T_{\varepsilon,i}/T_{\varepsilon,i}^0$.) Commonly, the absorption change is calculated as $\Delta\alpha_\varepsilon=-\ln(\langle T_{\varepsilon,i}\rangle/\langle T_{\varepsilon,i}^0\rangle)$ or $\Delta\alpha_\varepsilon=-\ln(\langle T_{\varepsilon,i}/T_{\varepsilon,i}^0\rangle)$. However, any noise in the detector signals will affect the ratio $p_{\varepsilon,i}/r_i$ more

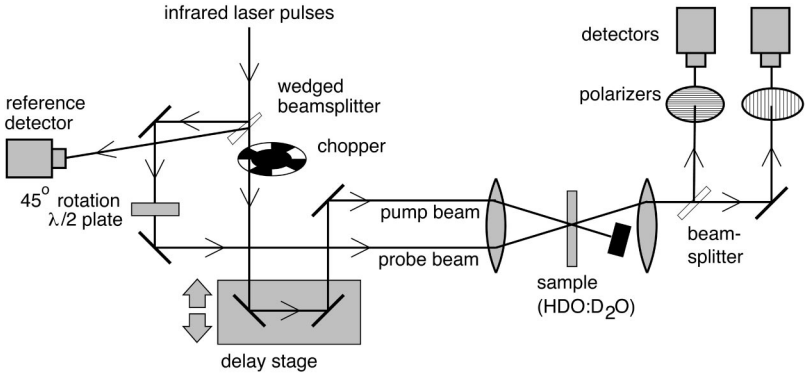

FIG. 3. Pump–probe setup. See the text for explanation.

strongly for pulses with a weaker energy. In the above equations, all laser shots are assigned equal weights, which causes excessive noise in $\Delta\alpha_\varepsilon$ due to pulses with low energies. Therefore, we calculate $\Delta\alpha_\varepsilon=-\ln(T_\varepsilon/T_\varepsilon^0)$, where T_ε and T_ε^0 result from a linear least squares fit of $p_{\varepsilon,i}=T_\varepsilon r_{\varepsilon,i}$ and $p_{\varepsilon,i}^0=T_\varepsilon^0 r_{\varepsilon,i}^0$ to the data, as is shown in Fig. 4, which leads to a strong reduction in the noise in $\Delta\alpha_\varepsilon$. The noise can be reduced even more by observing that, for a single laser shot, the numerator in Eq. (1) can be written as

$$\Delta\alpha_{\parallel,i}-\Delta\alpha_{\perp,i}=-\ln\left(\frac{p_{\parallel,i}}{p_{\perp,i}}\cdot\frac{p_{\perp,i}^0}{p_{\parallel,i}^0}\right), \tag{2}$$

which is now not influenced by any noise in the reference signals r_i. Using similar arguments as for $T_\varepsilon/T_\varepsilon^0$, we calculate the quantities D and D^0, that represent the ratios of the signals measured by the parallel and perpendicular detectors, by fitting the functions $p_\parallel=Dp_\perp$ and $p_\parallel^0=D^0p_\perp^0$. We can now express the rotational anisotropy from Eq. (1) as

$$R=\frac{-\ln(D/D^0)}{\Delta\alpha_\parallel+2\Delta\alpha_\perp}. \tag{3}$$

We found that the above techniques improved our signal to noise ratio by almost an order of magnitude, compared to mere averaging of the detector responses.

D. Sample

The sample consisted of a 500 μm thick layer of HDO in D_2O. The HDO concentration is chosen in such a way that the transmission at the center of the O–H absorption band was in the range 2%–8%. Thereby a compromise was achieved between detector signal to noise ratio and a maximum induced absorption change. This corresponds to a typical HDO concentration of 1%. The use of this low concentration has two purposes: First, the large distance between HDO molecules reduces any direct (Förster) energy transfer from one O–H group to another O–H group, which would lead to a rapid decay of the rotational anisotropy without actual orientational motion of the molecules.[6] Second, the low HDO concentration strongly reduces heating effects; we estimate the temperature increase per pulse to be less than 0.2 K, assuming that 20 μJ of energy are homogeneously dissipated in the $200^2\times500\,\mu\text{m}^3$ focus. To prevent accumulated local heating, we rotated the sample in order to get a fresh sample for every pump pulse. The sample temperature was stabilized within 1 K.

III. RESULTS

Figure 5 shows a typical measurement of the transmission changes $T_\varepsilon/T_\varepsilon^0$ and D/D^0 in HDO:D_2O as a function of the delay between the pump and probe pulses. We repeated these measurements as a function of both the temperature (in the range 298–362 K) and the pulse frequency (3400 and 3500 cm^{-1}). It can be calculated that this 20% relative transmission change corresponds to typically 3% of the O–H bonds being excited, which allows us to neglect saturation effects in the analysis in Sec. IV.

Due to scattered light from the pump pulses, the data in Fig. 5 have a significant background. As is clear from Eq. (3), any tiny background contribution will have a large effect on the value of the rotational anisotropy R. Since the bleaching decays with an 850 fs time constant,[7] the residual bleaching at $t=5$ ps is of the same magnitude as the error in the data points. In order to evaluate the background with the highest possible accuracy, we assumed an exponential decay of the raw T/T^0 values in Fig. 5 in the range 1.5–5 ps, such that we could use 10 data points instead of only one. The

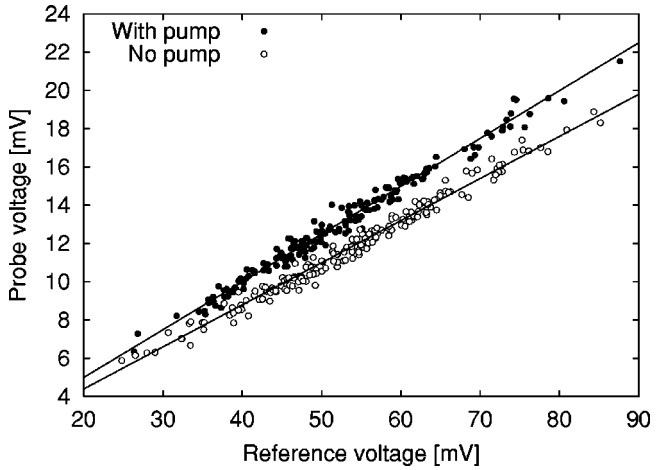

FIG. 4. Typical detector responses for the component of the probe polarization that is parallel to the pump polarization. The lines are linear least-squares fits to the data, with slope $T=\Sigma_i p_{\parallel,i}r_i/\Sigma_i r_i^2$ (similar for T_0).

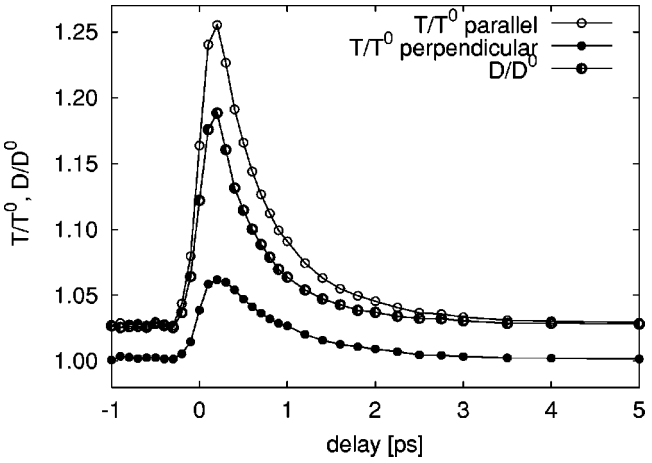

FIG. 5. Raw data of $T_{\parallel}/T_{\parallel}^{0}$, $T_{\perp}/T_{\perp}^{0}$, and D/D^{0}. The frequency was 3400 cm^{-1} and the temperature was 298 K. The different background levels are caused by scattered light from the pump pulses. The smooth increase of the signal around $t=0$ ps is caused by the nonzero pulse duration.

assumption of exponential decay is justified, since the resulting rotational anisotropy R in Fig. 6 decays exponentially for $t>1.5$ ps.

The data in Fig. 6 display several facts. First, this decay is faster in the experiments at 3500 cm^{-1} than in the experiments at 3400 cm^{-1}. Second, although the typical time scale of the relaxation is on the order of 1 ps, the decays are not exponential, which is visible at delay times less than 1.5 ps. Finally, the decay of the rotational anisotropy becomes faster as the temperature increases.

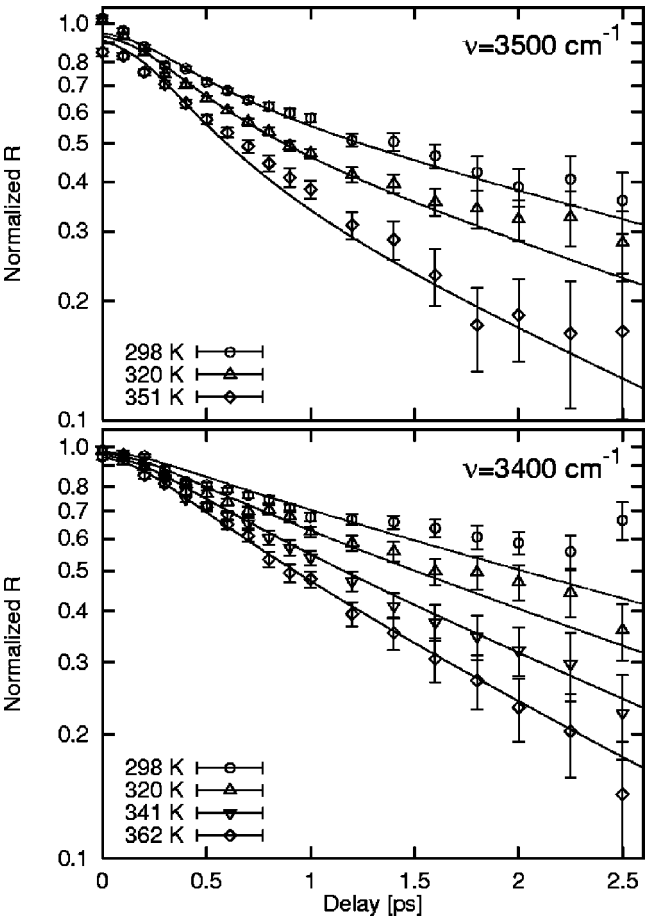

FIG. 6. The decay of the rotational anisotropy R in HDO:D_2O for a series of temperatures, measured at excitation frequencies 3400 and 3500 cm^{-1}. The data are normalized at $t=0$ ps. The lines represent our model calculations, discussed in Sec. IV.

IV. MODEL FOR ACTIVATED REORIENTATION IN LIQUID WATER

A. Model

The frequency dependence of the anisotropy decay suggests that the reorientation rate of an individual molecule depends on its resonance frequency. This can be expected in view of the relation between O–H stretch frequency and hydrogen bond strength (see Sec. I). A higher O–H vibration frequency implies a weaker hydrogen bond, which probably leads to a larger freedom for the O–H group to change its orientation. Since the decay of the anisotropy becomes faster at higher temperatures, it is likely that this reorientation can be described as an activated process. In order to change orientation, a molecule would need to overcome a potential barrier, which becomes easier when more thermal energy is available. For comparison, for a molecule as light as the HDO molecule, the thermal energy available at 298 K would correspond to a classical angular frequency on the order of 10 ps^{-1}. The much lower observed reorientation rate indicates that there is indeed a potential barrier present. Since it is likely that, in order to change its orientation, a water molecule must stretch or break the hydrogen bond, this activation energy E_{act} is expected to decrease with increasing O–H stretch frequency ν. The reorientation time should satisfy the Arrhenius equation

$$\frac{1}{\tau_{\mathrm{r}}(\nu)}=\frac{1}{\tau_0}\exp(-E_{\mathrm{act}}(\nu)/k_{\mathrm{B}}T). \tag{4}$$

Here, T is the temperature, k_{B} is Boltzmann's constant, and the pre-exponential constant τ_0 is an indication for the reorientation time in absence of any activation energies.

The above frequency dependence of the reorientation time τ_r cannot provide a complete description of the observed reorientation in water, since it was previously found that the O–H stretch frequencies of individual HDO molecules are rapidly varying within the O–H absorption band.[8,9] This spectral diffusion results from the stochastic modulation of the hydrogen bond length. We have to incorporate this spectral diffusion process into our model. We assume that the absorption line shape is given by

$$\exp(-(\nu-\nu_0)^2/2(\Delta\nu)^2), \tag{5}$$

where ν is the $v=0\rightarrow1$ transition frequency, $\Delta\nu$ defines the width of the absorption band, and ν_0 is the center of the absorption band. Furthermore, we assume that we can describe the spectral diffusion as a Gauss–Markov random process,[10] where $\delta\nu(t)=\nu(t)-\nu_0$ satisfies

$$\langle\delta\nu(t)\,\delta\nu(0)\rangle=(\Delta\nu)^2e^{-t/\tau_{\mathrm{s}}}. \tag{6}$$

Here, τ_s is the autocorrelation time constant for the detuning, which is a measure for the rate of spectral relaxation. The value of τ_s was found to be 500 fs in one study,[8] and 700 fs in another.[9]

The effective absorption of the probe pulse is influenced by both the stimulated emission from the excited $v=1$ state, and the absorption by the $v=0$ ground state. The spectrum for stimulated emission is shifted to a lower frequency (corresponding to shorter hydrogen bonds), compared to the absorption spectrum. This shift, approximately $60\,\mathrm{cm}^{-1}$,[8] can be predicted from the linewidth of the O–H stretch absorption band, and is commonly referred to as the dynamic Stokes frequency shift.

In this Gauss–Markov-type spectral diffusion, we can describe the response by assuming that the hydrogen bond is a Brownian oscillator. For this oscillator, it is possible to derive analytical expressions for the signals in pump–probe experiments.[11] However, the combination of spectral diffusion and a frequency-dependent reorientation rate is too complicated for an analytical treatment. Therefore, we used numerical methods to evaluate the reorientational dynamics.

The absorption changes in Eq. (1) depend on the difference in population of the vibrational ground and excited state before and after the pump pulse. If the effective population change in state v contributing to absorption of probe light at frequency ν and polarization ε is given by $\Delta n_{\varepsilon,v}$, then

$$\Delta\alpha_\varepsilon = -\rho\sigma(\Delta n_{\varepsilon,0}(\nu) - \Delta n_{\varepsilon,1}(\nu)). \tag{7}$$

Here, ρ is the density of HDO molecules and σ is the cross section for the radiative $v=0\rightarrow 1$ transition. Due to the Stokes shift, the spectral relaxation of the n_0 population differs from that of the n_1 population. Therefore, we need to consider these contributions separately. The measured rotational anisotropy is given by

$$R(t) = \frac{\int I_{\mathrm{probe}}(\nu,t) * [\Delta\alpha_\parallel(\nu,t) - \Delta\alpha_\perp(\nu,t)]\,d\nu}{\int I_{\mathrm{probe}}(\nu,t) * [\Delta\alpha_\parallel(\nu,t) + 2\Delta\alpha_\perp(\nu,t)]\,d\nu}, \tag{8}$$

where $I_{\mathrm{probe}}(\nu,t)$ is the power spectrum of the probe pulses at time t, the $*$ operator indicates time convolution, and the instantaneous absorption changes $\Delta\alpha_{\parallel,\perp}$ can be written as

$$\Delta\alpha_\parallel(\nu,t) - \Delta\alpha_\perp(\nu,t) = a_-(\nu,t) + b_-(\nu,t), \tag{9a}$$

$$\Delta\alpha_\parallel(\nu,t) + 2\Delta\alpha_\perp(\nu,t) = a_+(\nu,t) + b_+(\nu,t). \tag{9b}$$

The quantities $a_\pm$ and $b_\pm$ correspond to the contributions of the n_0 and n_1 populations, respectively [e.g., $a_- = -\rho\sigma(\Delta n_{0,\parallel} - \Delta n_{0,\perp})$]. We will not consider vibrational relaxation, since this does not affect the value of R. The excitation by the pump pulse, spectral diffusion, and reorientation, affect $a_\pm$ and $b_\pm$ according to the partial differential equations

$$\frac{\partial a_-}{\partial t} = \frac{2}{5} I_{\mathrm{pump}}(\nu,t) + \mathcal{D}_0 a_- - \frac{a_-}{\tau_r(\nu)}, \tag{10a}$$

$$\frac{\partial b_-}{\partial t} = \frac{2}{5} I_{\mathrm{pump}}(\nu,t) + \mathcal{D}_1 b_- - \frac{b_-}{\tau_r(\nu)}, \tag{10b}$$

$$\frac{\partial a_+}{\partial t} = I_{\mathrm{pump}}(\nu,t) + \mathcal{D}_0 a_+, \tag{10c}$$

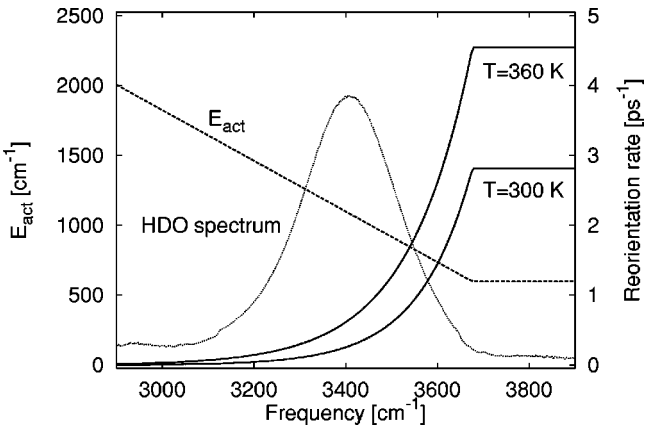

FIG. 7. Reorientation rate (defined as $1/\tau_r$) at 300 and 360 K (solid lines), the rotational activation energy as a function of the OH stretch frequency (dashed line), and the OH absorption band (dotted line).

$$\frac{\partial b_+}{\partial t} = I_{\mathrm{pump}}(\nu,t) + \mathcal{D}_1 b_+. \tag{10d}$$

Here, $I_{\mathrm{pump}}(\nu,t)$ is the normalized pump intensity (the absolute magnitude is not relevant, since this does not affect the value of R). The operators $\mathcal{D}_0$ and $\mathcal{D}_1$ describe spectral diffusion in the $v=0$ and $v=1$ states, respectively, and satisfy Eq. (6) (see Appendix). The coefficient 2/5 in Eqs. (10a)–(10b) ensures that the initial anisotropy is 2/5 in absence of spectral diffusion and orientational relaxation. Equations (10) are integrated numerically, with $a_\pm(\nu,t) = b_\pm(\nu,t) = 0$ for $t \ll 0$. Using the solutions of Eqs. (10), we calculate the decay of the measured anisotropy R in Eq. (8). We find that the experimental data can be well described if the activation energy E_{act} depends on the frequency as

$$E_{\mathrm{act}}(\nu) = \begin{cases} 600 + 1.81(3675 - \nu) & (\nu \leqslant 3675) \\ 600 & (\nu \geqslant 3675) \end{cases}, \tag{11}$$

where E_{act} and ν are expressed in cm^{-1} units. The constant of $600\,\mathrm{cm}^{-1}$ corresponds to the activation energy caused by effects such as steric hindering and other hydrogen bonds that do not affect the O–H stretch frequency. The $3675\,\mathrm{cm}^{-1}$ cut-off frequency is approximately equal to the gas-phase frequency where no D–O–H$\cdots$O hydrogen bond is present. Furthermore, the pre-exponential time constant $\tau_0 = 20$ fs, which is of the same order as the 100 fs gas-phase thermal rotation time.

The resulting frequency and temperature dependence of the reorientation rate is shown in Fig. 7. Clearly, this reorientation rate increases rather steeply around $3590\,\mathrm{cm}^{-1}$. It is not possible to describe the experimental results with a smoother frequency dependence of the reorientation rate. Further, we describe the spectral diffusion with a $60\,\mathrm{cm}^{-1}$ Stokes redshift and a spectral relaxation time $\tau_s = 500$ fs, in agreement with earlier results.[8] The resulting decays of the anisotropy are shown in Fig. 6.

B. Discussion of the model

For very small delays ($t < 0.2$ ps), the anisotropy decays more slowly than at larger delays, both in the calculations

TABLE I. Reorientation times after equilibration of the transient spectrum for the $v=0$ and $v=1$ vibrational states, calculated from the model.

T (K)	$\tau_{r,\mathrm{eq}}(v=0)$ (ps)	$\tau_{r,\mathrm{eq}}(v=1)$ (ps)
298	2.59	4.16
320	1.98	3.04
341	1.59	2.36
351	1.45	2.12
361	1.32	1.90

and the experiment. This is simply due to the fact that for these small delays, the creation of ''new anisotropy'' by the pump pulse compensates the decay of anisotropy due to reorientation. In addition, it can be expected that during the temporal overlap between pump and probe pulses around $t=0$ ps, coherent coupling effects cause an additional contribution to the anisotropy signal. Although there appears to be no coherent peak in the anisotropy, no definite conclusions about the reorientation should be drawn from the data around zero delay.

At delays <1.5 ps, the anisotropy decay strongly depends on frequency. At 3500 cm^{-1}, most excited molecules will initially be in the fast-reorienting part of the spectrum and thus cause a relatively high anisotropy decay rate. At 3400 cm^{-1}, the initial decay rate is only slightly faster than the average decay rate that is effective at larger delays (i.e., $t>1.5$ ps). At these larger delays, the absolute value of the anisotropy will be systematically lower at the high-frequency, fast-reorienting part of the spectrum, but the anisotropy decay rate will be identical throughout the spectrum. In other words, the spectrum of $\Delta\alpha_{\parallel}+2\Delta\alpha_{\perp}$ in the denominator of Eq. (8) does not change, and in the numerator, the spectrum of $\Delta\alpha_{\parallel}-\Delta\alpha_{\perp}$ only changes in amplitude. This final decay rate depends on the spectral relaxation constant, the fraction of molecules with a large reorientation rate, and the maximum value of the reorientation rate at the high-frequency side of the spectrum (which increases with temperature). This final decay of the anisotropy is determined by both the anisotropy decay of the $v=0$ state and that of the $v=1$ state. The fraction of fast-reorienting molecules in the $v=1$ state [the $b_{\pm}$ components in Eqs. (9)] is smaller than the fraction of fast-reorienting molecules in the $v=0$ state (the $a_{\pm}$ components), due to the Stokes red-shift in the $v=1$ spectrum. This results in slightly different anisotropy decay rates for these two contributions to the anisotropy signal.

To summarize, there are three time constants that contribute to the anisotropy decay at a given frequency and temperature. The first time constant is the inverse of the reorientation rate at the excitation frequency and mainly affects the decay at smaller delays. The value for this time constant can be read from Fig. 7. The second and the third time constants $\tau_{\mathrm{r,eq}}(v=0)$ and $\tau_{\mathrm{r,eq}}(v=1)$, that determine the decay at larger delays, are the reorientation time constants for the $v=0$ and $v=1$ states, respectively, after equilibration of the shape of the transient spectrum. By calculating the a and b contributions in Eq. (9) separately, we found the time constants for these slow processes as shown in Table I.

From Fig. 7, it is clear that only O–H groups with a weak hydrogen bond are able to change orientation. This implies that a molecule with a low O–H frequency and a strong hydrogen bond can only change orientation if the hydrogen bond is temporarily stretched, which corresponds to spectral diffusion to higher frequencies. In other words, only spectral diffusion enables these low-frequency molecules to change their orientation.

In our model, we have used the 500 fs time constant for spectral relaxation from Ref. 8. However, it is possible to describe our data with the 700 fs time constant measured by Gale *et al.*[9] In that case, we find a sligthly different activation energy, resulting in a reorientation rate curve in Fig. 7 that is shifted to the lower frequencies by less than 10 cm^{-1}. This shows that the model is not extremely sensitive to the spectral relaxation time constant.

Although our model can account well for both the frequency and the temperature dependence of the anisotropy decay, some refinements of the model are still possible. First, it is known that the O–H stretch absorption line shape changes with temperature.[12] In principle, this could be accounted for by modifying the spectral diffusion operators in Eqs. (10). Second, we assume that there is a single, well-defined, activation energy at a given O–H stretch frequency. However, this activation energy may very well depend on the strength of the other hydrogen bonds to other neighboring water molecules. Therefore, it would be more correct to assume a distribution of activation energies (and a resulting distribution of reorientation rates) at each frequency. Finally, in our model we explicitly account for the fact that the reorientation of the water molecules is enabled by the spectral diffusion. However, we do not take into account that in turn the spectral diffusion may be affected by the reorientation. When an O–H group changes its orientation, it is likely that the length of its hydrogen bond will change simultaneously. In other words, reorientation by itself contributes to spectral diffusion. In principle, the model could be refined by assuming that the spectral diffusion time constant has a frequency-dependence that is linked to the reorientation time constant, e.g., $1/\tau_{\mathrm{diff}}(\nu)=1/\tau_{\mathrm{min}}+A/\tau_{\mathrm{r}}(\nu)$, where τ_{min} and A are to be determined from our data. However, this refinement will have little effect, since the reorientation is very slow and takes place on a much slower time scale than the spectral diffusion, whereas at high frequencies, the hydrogen-bond length is large and any rotations will not strongly influence the frequency of an OH vibration. In addition, the spectral relaxation in water can be well described as a Gauss–Markov process, as was shown by ourselves[8] and by Gale *et al.*[9] This means that there is no evidence for a significant frequency dependence of spectral diffusion.

C. Comparison with other studies

In a previous publication,[1] time constants τ_{r} of 0.7 and 13 ps were obtained with the same method as presented here. The 0.7 ps time constant corresponds to a spectral average of the initial fast process at the high-frequency side of the spectrum (approximately 1 ps), while the 13 ps time constant corresponds to the slower time constants $\tau_{\mathrm{r,eq}}(v=0)=2.6$ ps and $\tau_{\mathrm{r,eq}}(v=1)=4.2$ ps that result after equilibra-

tion of the transient spectral line shapes. The time constants differ from the earlier results as a result of the improved signal to noise ratio.

For comparison of reorientational time constants calculated or measured with other methods, it should be noted that there is a difference between the first- and second-order reorientation times τ_1 and τ_2. The time constant τ_1 is the decay time of the first-order correlation function $C_1(t) = \langle \mathbf{e}(t) \cdot \mathbf{e}(0) \rangle$, where $\mathbf{e}$ denotes a unit vector in the molecular frame. The time constant τ_2 is the decay time of the second-order correlation function $C_2(t) = \langle P_2(\mathbf{e}(t) \cdot \mathbf{e}(0)) \rangle$, where $P_2(x)$ is the second Legendre polynomial in x. For situations where the reorientation is isotropic, i.e., there is no preferred rotation axis or molecular orientation, the time constants relate as $\tau_1 = 3\tau_2$. The reorientation time τ_r in this study corresponds to τ_2 with $\mathbf{e}$ directed along the O–H bond.

As a first comparison, we can examine the Debye–Stokes equation $\tau_2 = 4\pi a^3 \eta / k_B T$ for a spherical particle, where a is the hydrodynamic radius of a water molecule and η is the viscosity of water. Using $\eta = 8.9 \times 10^{-4}$ Pa s for H_2O (Ref. 13) and $\tau_2 = \tau_{r,eq}(v=0) = 2.59$ ps, we find that $a = 1.0$ Å. This classically obtained result compares surprisingly well to the estimate $a = 1.9$ Å that follows from the bulk density of water.

The reorientational dynamics of liquid water have also been investigated with molecular dynamics simulations. These calculations yield time constants that depend strongly on the simulation method. In *ab initio* density functional theory calculations, values for τ_2 have been reported that range from 1.2 to 9 ps.[14] In classical molecular dynamics studies, time constants between 0.7 and 1.7 ps were found.[15,16] In one study, a biexponential decay of $C_2(t)$ was found with 1.0 and 13 ps time constants.[17]

Our values for $\tau_{r,eq}(v=0)$ compare very well to data from nuclear magnetic resonance (NMR) and dielectric relaxation measurements. In the NMR studies, the reorientation time τ_2 can be calculated from the relaxation time (typically tens of seconds) of the hydrogen nuclei spins in water. The reorientation times in H_2O were estimated to be 2.6 and 0.9 ps at 298 K and 350 K, respectively.[18] In dielectric measurements, the alignment time of the dipole moment of water molecules to a THz electric field is measured. Both in H_2O and D_2O, the Debye time τ_1 varies from 8 ps at 300 K to 3 ps at 360 K,[19–21] which corresponds to 2.7 and 1.0 ps, respectively, for τ_2. Hence, the time constants found in NMR and dielectric relaxation measurements are in excellent agreement with the value of $\tau_{r,eq}(v=0)$ that we observe after the transient spectrum has equilibrated. This $\tau_{r,eq}(v=0)$ represents an effective reorientation time scale that forms an average over *all* water molecules. An important advantage of the femtosecond nonlinear spectroscopic method employed in this work is that the reorientational dynamics of only a *subensemble* of the water molecules can be investigated. This enables a determination of the mechanism behind the effective reorientation time of liquid water as observed in NMR and dielectric relaxation experiments. This work shows that the effective reorientation rate in liquid water is governed by the fraction of water molecules for which reorientation is not hindered by the O–H···O hydrogen bond, the rate of this unhindered reorientation, and the rate at which the strength of the hydrogen bonds is stochastically modulated.

V. CONCLUSIONS

We have measured the orientational relaxation of HDO molecules dissolved in liquid D_2O by creating an anisotropic population of excited O–H stretch vibrations with femtosecond mid-infrared pulses and by subsequently measuring the decay of this anisotropy. The decay of the anisotropy is nonexponential and takes place on a typical time scale of 1 ps. At the blue side of the inhomogeneously broadened O–H stretch vibration absorption band ($3500\,\mathrm{cm}^{-1}$), the anisotropy decays faster than at the center of the absorption band ($3400\,\mathrm{cm}^{-1}$).

We find that the frequency and temperature dependence of the anisotropy decay can be well described with a model in which the reorientation is an activated process. The activation energy for reorientation decreases linearly with increasing hydrogen-bond length. This yields a reorientation rate as a function of frequency that increases steeply. By varying the temperature, we find that the maximum reorientation rate at the high-frequency side of the absorption band increases from $2.8\,\mathrm{ps}^{-1}$ at 298 K to $4.5\,\mathrm{ps}^{-1}$ at 360 K.

The model also includes the effects of spectral diffusion that results from the stochastic modulation of the hydrogen-bond length. It is found that the reorientation of strongly hydrogen-bonded water molecules is enabled by the weakening of the hydrogen bond.

ACKNOWLEDGMENTS

The work described in this paper is part of a collaborative research program of NIOK (Netherlands Graduate School of Catalysis Research) and FOM (Foundation for Fundamental Research on Matter), which is financially supported by NWO (Netherlands Organization for the Advancement of Research). We thank Wim van der Zande and Marc Vrakking for their helpful comments.

APPENDIX: OPERATORS FOR SPECTRAL DIFFUSION

The operator $\mathcal{D}$ for spectral diffusion in Eqs. (10) should have the property that the line shape of a population spectrum $n(\nu)$ will relax to the line shape of the equilibrium absorption spectrum $A(\nu)$. The local flux of population $\varphi(\nu)$ from a frequency directly below ν to a frequency directly above ν satisfies

$$\varphi(\nu) = -D \frac{\partial}{\partial \nu} \left(\frac{n(\nu)}{A(\nu)} \right), \tag{A1}$$

where D is the diffusion constant. For a completely flat absorption spectrum (constant A), this is equivalent to the standard diffusion equation $\partial n / \partial t = D \partial^2 n / \partial \nu^2$. We assume that for the ground state operator $\mathcal{D}_0$, the equilibrium spectrum $A(\nu)$ is the CW absorption spectrum, and for the excited state operator $\mathcal{D}_1$, $A(\nu)$ is redshifted by $60\,\mathrm{cm}^{-1}$, corre-

sponding to the Stokes shift. In the numerical computations, $n(\nu)$ was a discrete distribution to which the above equation was applied directly.

[1] S. Woutersen, U. Emmerichs, and H. J. Bakker, Science **278**, 658 (1997).
[2] R. Laenen, C. Rauscher, and A. Laubereau, J. Phys. Chem. B **102**, 9304 (1998).
[3] A. Novak, Struct. Bonding (Berlin) **18**, 177 (1974).
[4] U. Emmerichs, S. Woutersen, and H. J. Bakker, J. Opt. Soc. Am. B **14**, 1480 (1997).
[5] H. Graener, G. Seifert, and A. Laubereau, Chem. Phys. Lett. **172**, 435 (1990).
[6] S. Woutersen and H. J. Bakker, Nature (London) **402**, 507 (1999).
[7] H. K. Nienhuys, S. Woutersen, R. A. van Santen, and H. J. Bakker, J. Chem. Phys. **111**, 1494 (1999).
[8] S. Woutersen and H. J. Bakker, Phys. Rev. Lett. **83**, 2077 (1999).
[9] G. M. Gale, G. Gallot, F. Hache, N. Lascoux, S. Bratos, and J.-C. Leickman, Phys. Rev. Lett. **82**, 1068 (1999).
[10] R. Kubo, M. Toda, and N. Hashitsume, *Statistical Physics II: Nonequilibrium Statistical Mechanics* (Springer-Verlag, Berlin, 1995).
[11] S. Mukamel, *Principles of Nonlinear Optical Spectroscopy* (Oxford University Press, Oxford, 1991).
[12] T. A. Ford and M. Falk, Can. J. Chem. **46**, 3579 (1968).
[13] *CRC Handbook of Chemistry and Physics*, 75th ed., edited by D. R. Lide (Chemical Rubber, Boca Raton, 1994).
[14] M. Sprik, J. Hutter, and M. Parrinello, J. Chem. Phys. **105**, 1142 (1996).
[15] A. Chandra and T. Ichiye, J. Chem. Phys. **111**, 2701 (1999).
[16] D. van der Spoel, P. J. van Maaren, and H. J. C. Berendsen, J. Chem. Phys. **108**, 10220 (1998).
[17] Y.-L. Yeh and C.-Y. Mou, J. Phys. Chem. B **103**, 3699 (1999).
[18] D. W. G. Smith and J. G. Powles, Mol. Phys. **10**, 451 (1966).
[19] J. T. Kindt and C. A. Schmuttenmaer, J. Phys. Chem. **100**, 10373 (1996).
[20] C. Rønne, L. Thrane, P.-O. Åstrand, A. Wallqvist, K. V. Mikkelsen, and S. R. Keiding, J. Chem. Phys. **107**, 5319 (1997).
[21] C. Rønne, P.-O. Åstrand, and S. R. Keiding, Phys. Rev. Lett. **82**, 2888 (1999).